Three dominant *Vibrio cholerae* lytic phage all require O1 antigen for infection

Drew A. Beckman and Christopher M. Waters*

Department of Microbiology and Molecular Genetics, Michigan State University, East Lansing, Michigan, USA, 48824

Running Title: *V.c.* O-Antigen Mutants Pan-Resistant to ICP Phage

***Corresponding Author:**

5180 Biomedical and Physical Sciences

567 Wilson Road

East Lansing, MI 48824

Telephone 517-884-5360

E-mail: watersc3@msu.edu

Keywords:

SUMMARY

In its natural aquatic environment, the bacterial pathogen *Vibrio cholerae*, the causative agent of the enteric disease cholera, is in constant competition with bacterial viruses known as phages. Following ICP3 infection, *V. cholerae* cultures that exhibited phage killing always recovered overnight, and clones isolated from these regrowth populations exhibited complete resistance to subsequent infections. Whole genome sequencing of these resistant mutants revealed seven distinct mutations in genes encoding for enzymes involved in O1 antigen biosynthesis, demonstrating that the O1 antigen is a previously uncharacterized receptor of ICP3. To further elucidate the specificity of the resistance conferred by these mutations, they were

challenged with the *V. cholerae*-specific phages ICP1 and ICP2. Despite no prior exposure to these phages, all seven O1 antigen mutants demonstrated pan-resistance to all three ICP phages. Given that the O1 antigen is required for infection of *V. cholerae,* our results show that the ICP phage have evolved to recognize an essential surface molecule for infection, providing a barrier to the evolution of pathogenic *V. cholerae* phage resistance in natural environments.

MAIN

Introduction

The Gram-negative aquatic pathogen *Vibrio cholerae*, the causative agent of the severe enteric diarrheal disease cholera, is primarily found in the saline conditions of estuaries and brackish water (1). Recent estimates from 2015 place the human burden of disease worldwide in the range of 1.3-4.0 million cases and approximately 95,000 deaths annually as a result of rapid dehydration (2). Countries in sub-Saharan Africa and southern Asia are most directly impacted by cholera, but natural and manmade humanitarian disasters have ignited outbreaks in Haiti and Iraq (3, 4). Cholera is undoubtedly worsened by poverty where water treatment systems are suboptimal or non-existent (5).

Within its environment, *V. cholerae* is preyed upon by bacterial viruses known as bacteriophages, or phages, and these parasites are significant drivers of *V. cholerae* evolution (6). Lytic phages commandeer the host cell's machinery and replicate to high numbers, eventually lysing the host cell. This predation is a critical driver of co-evolution among *V. cholerae* bacteria and their respective phages, applying selective pressure for the evolution of phage defense mechanisms like abortive infection (7), mobile genetic elements (8), and toxin-antitoxin systems (9) in addition to counter-defense systems evolved by the phage (10). Despite this robust phage defense, there are three major *V. cholerae* specific lytic phage families isolated from patient stool samples at the International Center for Diarrheal Disease Research, Bangladesh known as ICP1, ICP2, and ICP3 (11, 12). These three phages, while identified

53 together, are quite diverse; ICP1 is a member of the *Myoviridae* family and has a genome 2-3
54 times larger than ICP2 and ICP3 which are members of the *Podoviridae* family (12). The ICP
55 phages are the three largest of the nine major phage families that have been identified to infect
56 *V. cholerae* (13).

57 Before phage can successfully infect host bacteria, they must first bind to a specific cell
58 surface receptor that determines phage specificity and host range. The receptor targeted by
59 ICP1 to mediate phage invasion and replication is the O1 antigen in the lipopolysaccharide
60 (LPS) of the *V. cholerae* outer membrane (11, 12). Of the over 200 known serogroups, only O1
61 and O139 are pathogenic with the former responsible for the greatest number of cases (11, 14,
62 15). The El Tor biotype of *V. cholerae,* which is responsible for the current seventh cholera
63 pandemic, can be subdivided into serotypes based on methylation of the O1 antigen. The
64 Ogawa serotype is categorized by an additional methyl group on the most distal perosamine
65 monomer while this methyl is absent in the Inaba serotype (4, 14, 15). The principal receptor for
66 ICP2 is the OmpU outer membrane porin (16). However, the receptor for ICP3 remains
67 uncharacterized (3, 17). These structures are excellent targets for phage exploitation because
68 of their key roles in human pathogenesis and antimicrobial resistance. For instance, OmpU is
69 required for efficient colonization of hosts while O1 antigen deficient *V. cholerae* mutants are
70 more sensitive to the antibiotic polymyxin B as well as the bactericidal/permeability increasing
71 (BPI) antimicrobial peptide secreted by the human gut (18, 19).

72 Understanding the interaction between the ICP phages and *V. cholerae* is not only
73 essential for characterizing the evolution and ecology of *V. cholerae* in its natural environments,
74 but also for the effective development of new cholera treatment strategies. Phage therapy is
75 emerging as an effective complement to antibiotic treatment, especially with the rise of antibiotic
76 resistant strains (20–22). The phage tropism for its individual receptor limits the negative effects
77 on the human host and their microbiome (23). Two phage therapy approaches are being
78 developed to treat cholera including the Phi_1 phage (24) and a cocktail of ICP1, ICP2, and

ICP3 (3). Therefore, identifying the receptors of these phage has important clinical ramifications.

Here, we used a forward genetics approach to identify the previously unknown ICP3 receptor by examining several *V. cholerae* escape mutants following ICP3 infection. Our results showed that O1 antigen biosynthesis enzymes were mutated in all ICP3 resistant strains, and surprisingly these mutants exhibited pan-resistance to ICP1, ICP2, and ICP3, demonstrating that the O1 antigen is a conserved receptor for all three ICP phages.

Results

Isolation of ICP3 resistant *V. cholerae*

During experiments studying the interaction of ICP3 phage with two newly discovered *V. cholerae* phage defense systems (7, 9), we observed that after an initial sharp decrease in the culture optical density upon ICP3 addition to values nearly equivalent to blank media controls, the bacterial cultures always rebounded to densities resembling the uninfected cultures. To establish the growth kinetics of *V. cholerae* in liquid media infected with ICP3 phage, an overnight culture of WT cells was subcultured into ten replicates, five of which were subsequently infected with ICP3 during mid-exponential growth phase at a multiplicity of infection (MOI) of 1.0 and the other five at 0.1 (Fig. 1). The density of the cultures rapidly decreased to initial inoculum levels 0.75 hr or 1.0 hr after ICP3 addition with 1.0 MOI or 0.1 MOI, respectively (Fig. 1). However, the OD_{600} of these cultures began to rebound 2 to 3 hr following the maximal drop. 24 hours later, the infected and uninfected cultures exhibited nearly identical optical densities (Fig. 1).

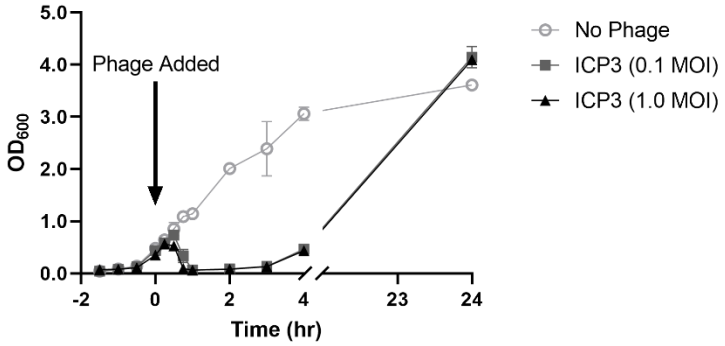

Figure 1: Infected *V. cholerae* cultures spontaneously recover over time.

Growth curves of WT *V. cholerae* cultures challenged with ICP3 phage at varying multiplicities of infection (MOI). ICP3 phage were added at 0 hr as indicated by the arrow. Data points are the mean of five biological replicates in the case of the phage groups (n = 5), and two in the case of the no phage control (n = 2). Error bars represent the standard deviation.

We hypothesized that the cells able to propagate in the phage-infected cultures were escape mutants resistant to ICP3. We isolated an individual clone from each of the ten independent overnight cultures that had rebounded from ICP3 infection. Each isolate was rechallenged with ICP3 at the original MOI of 1.0 for A-E (Fig. 2A) and 0.1 for F-J (Fig. 2B). Four of the five isolates infected with an MOI of 1.0 were resistant to ICP3 phage predation (Fig. 2A) while all five isolates challenged at an MOI of 0.1 were able to withstand ICP3 reinfection (Fig. 2B).

A

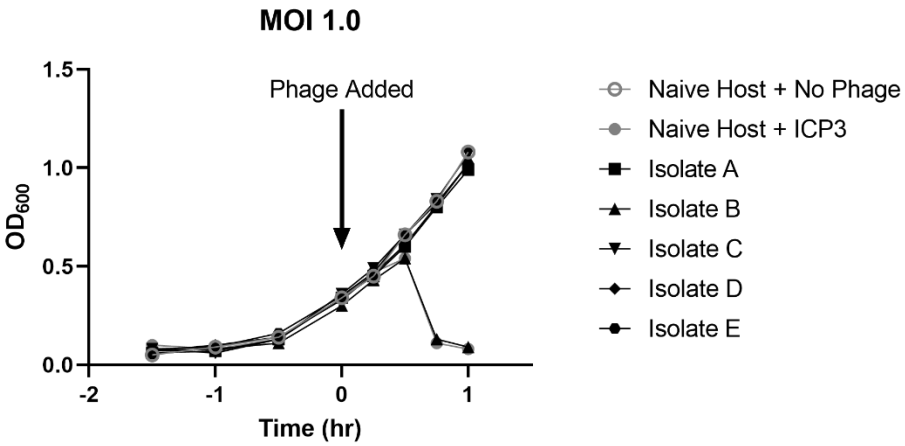

B

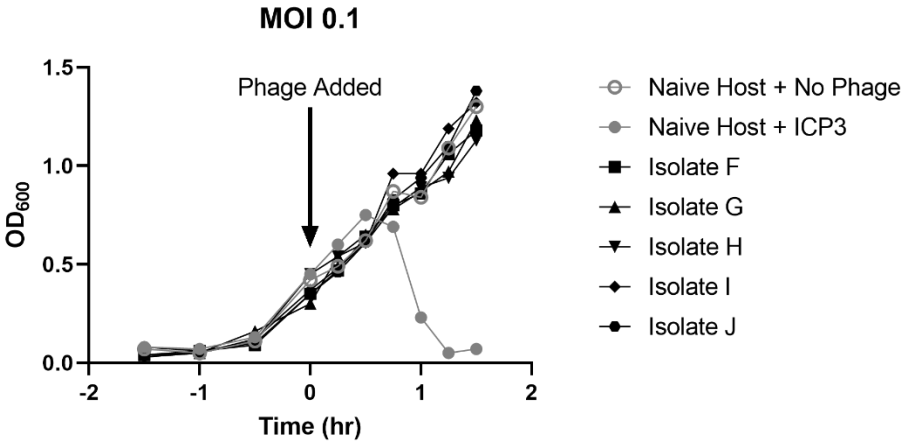

Figure 2: Recovered isolates demonstrate resistance to ICP3 phage in liquid culture. From the recovery pools of cultures that rebounded from ICP3 phage infection, individual isolates were obtained and rechallenged in a similar manner. They were either infected at an MOI of 1.0 (A) or 0.1 (B) based on their original recovery pool. ICP3 phage, or SM buffer in the case of the no phage control, was added at 0 hr as indicated by the arrow.

Resistant mutations are in O1 antigen biosynthesis genes

Whole genome sequencing of all nine resistant isolates identified that isolates A-I (excluding the non-resistant isolate B) shared the same 11 bp deletion in the *manB* gene while isolate J had an insertion in the *wbeU* gene (Table 1, Fig. 3). Both genes are part of the O1 antigen biosynthesis operons of *V. cholerae* (14, 25). Given that the identical mutation in *manB* was isolated from 8 independent cultures, we hypothesized this mutation was likely present in the original common starting overnight culture. Therefore, to isolate additional resistance mutations, five independent overnight cultures of WT *V. cholerae* were inoculated using individual colonies and subjected to ICP3 infection at an MOI of 1.0. All five cultures exhibited regrowth after the initial population decline. Individual clones from these five populations that were resistant to ICP3 rechallenge were isolated and their genomes were sequenced (isolates K-O). In each isolate, there was only one unique mutation, all of which mapped to the O1 antigen biosynthesis pathway (Table 1, Fig. 3). Importantly, no other resistant mutations outside of the O1 biosynthesis genes were isolated. These seven unique ICP3 resistant mutants in the O1 antigen biosynthesis pathway were present in six different genes. Six of these mutations are likely null either by causing frameshift mutations (isolates A, J, L, N, and O) or a significant deletion (isolate K) while isolate M has a missense mutation in *gmd* (Table 1). Given the localization of these resistance-conferring mutations, we conclude that ICP3 requires the O1 antigen for infection of *V. cholerae*.

Table 1: Whole Genome Sequencing of Pan-Resistant Isolates Reveals Mutations in the O-Antigen Biosynthesis Pathway

Isolate	Gene[a]	Position[b]	Location In Gene	Mutation	Protein Product[c]
A, C-I	***manB***, *VC0242*	Chr I. 2,696,238	920-930/1392 nt	Δ11 bp	Phosphomannomutase
J	***wbeU***, *rfbU*, *VC0259*	Chr I. 2,681,562	571/1113 nt	+G	Glycosylyltransferase / LPS Biosynthesis Protein
K	***wbeN***, *rfbN*, *VC0251*	Chr I. 2,687,710	78-95/2478 nt	Δ18 bp	Acyl-CoA Reductase / Acyl Protein Synthase
L	***wbeN***, *rfbN*, *VC0251*	Chr I. 2,685,438	2367/2478 nt	+5 bp	Acyl-CoA Reductase / Acyl Protein Synthase
M*	***gmd***, *VC0243*	Chr I. 2,695,683	91/1122 nt	G→A (H31Y)	GDP-Mannose 4,6-Dehydratase / Oxidoreductase
N	***manC***, *VC0241*	Chr I. 2,698,253	315/1398 nt	ΔC	Mannose-1-Phosphate Guanylyltransferase / Mannose-6-Phosphate Isomerase
O	***wbeM***, *VC0250*	Chr I. 2,688,092	828/1125 nt	+A	Iron-containing Alcohol Dehydrogenase

[a]Gene names were determined as part of the *wbe* cluster (14, 15, 25) and the *rfb* cluster (27, 36).

[b]NZ_CP046844 (Chr I) and NZ_CP046845 (Chr II) used as reference genomes.

[c]Putative enzyme functions based on these reference genomes as well as Pombo *et al*, 2022 where applicable (37).

*Demonstrated partial resistance in solid culture.

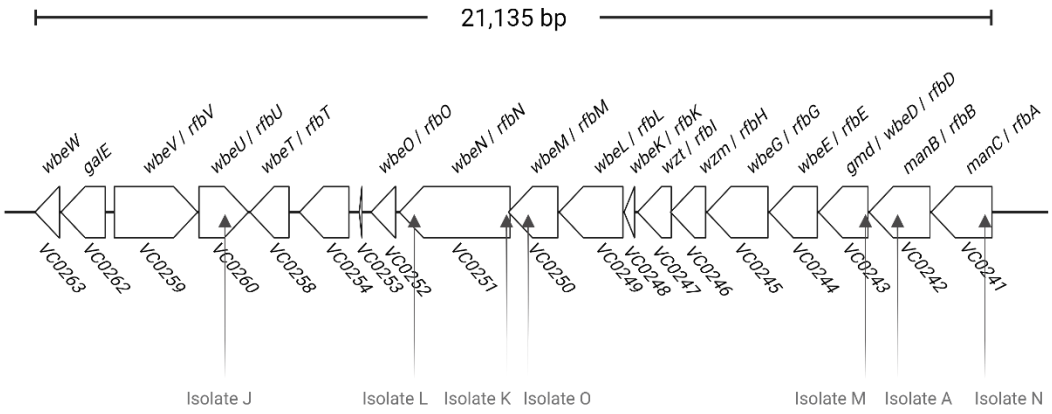

Figure 3: O1 antigen biosynthesis pathway genes indicating sites of mutations in resistant isolates.

Diagram depicting the genes of the *wbe* locus (*rfb* locus) in O1 serotypes of *V. cholerae* strains.

The block arrows of each gene point in the direction of transcription with gene sizes drawn to scale. Multiple names of each gene are given where applicable. The total length from the start codon of *VC0241* to the stop codon of *VC0263* is provided. Vertical arrows indicate the location of mutations in the individual isolates identified by whole genome sequencing.

ICP3 resistant mutants are also resistant to ICP1 and ICP2 infection

To investigate if these seven ICP3 resistant mutants demonstrated cross-resistance to ICP1 and ICP2, they were grown in liquid culture to exponential phase and exposed to ICP1, ICP2, or ICP3. In these conditions, all the resistant mutants grew similar to the WT strain in the absence of phage (Fig. 4A) and were resistant to ICP3 infection (Fig. 4D). Interestingly, all seven ICP3 resistant mutants were also completely resistant to ICP1 ($p < 0.0001$) and ICP2 ($p < 0.0001$) infection in liquid infection assays (Figs. 4B, C).

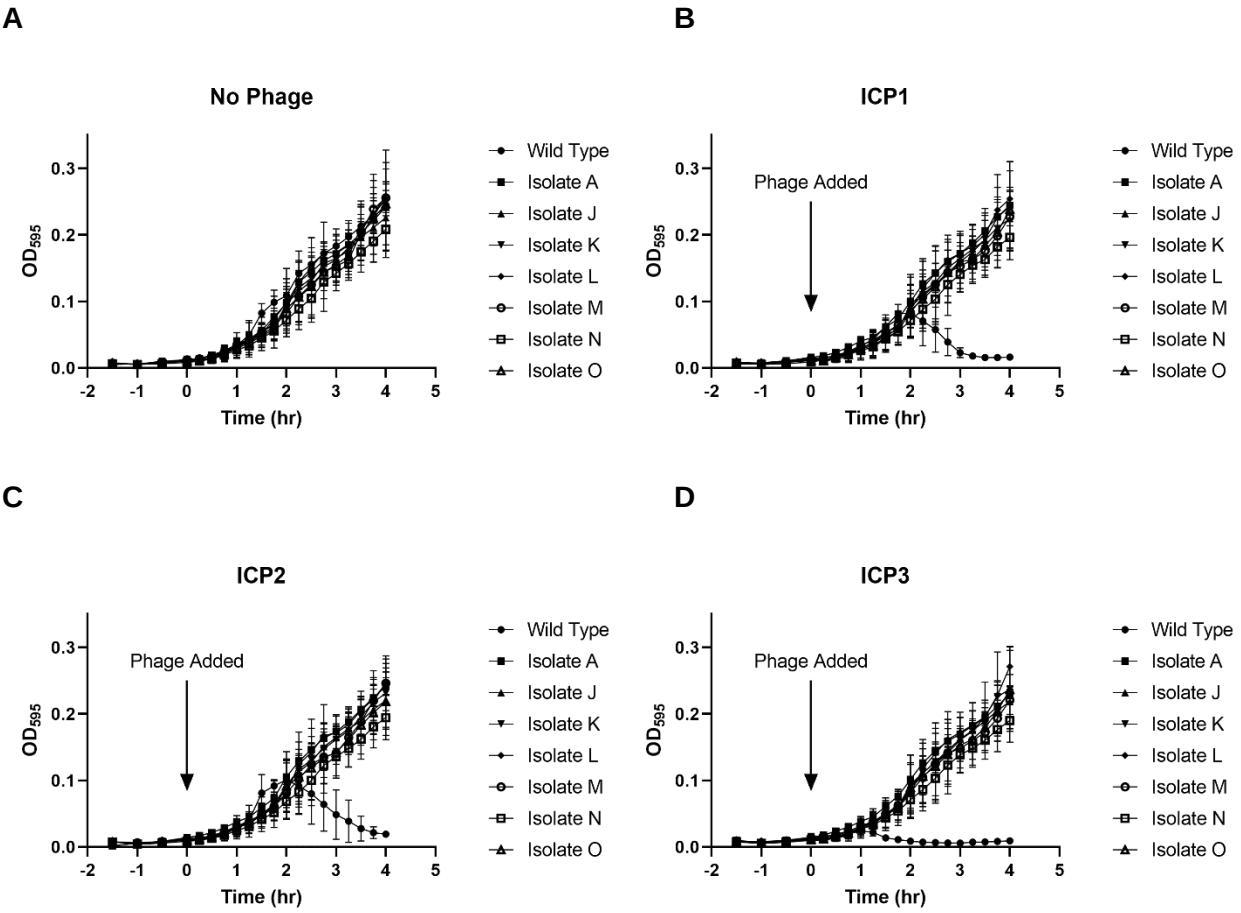

Figure 4: All ICP3 resistant mutants were pan-resistant to ICP1 and ICP2 in liquid culture. Growth curves for each ICP3 resistant mutant in the presence of no phage (A), ICP1 (B), ICP2 (C), and ICP3 (D) in liquid culture. Phage were added at 0 hr as indicated. The average of three biological replicates is shown for each strain (n = 3). Error bars represent the standard deviation. Two-Way Repeated Measures ANOVA was performed with Dunnett's post-hoc multiple comparisons tests between each strain. Significance at the final time point was $p < 0.0001$ for each strain compared to the WT control when phage was added (B-D). There was no significant difference between strains in the no phage condition (A).

To further examine ICP resistance in a different environment, the seven resistant mutants were tested in an efficiency of plaquing (EOP) assay for the ability to form plaques on a

211 solid medium. An example of this plaquing assay for both the sensitive WT control and Isolate A
212 is shown (Fig. 5A). Of the seven previously resistant *V. cholerae* mutants, six were completely
213 resistant to ICP1 ($p = 0.0005$), ICP2 ($p < 0.0001$), and ICP3 ($p = 0.0012$) showing no plaques at
214 any dilution of phage tested (Figs. 5B-D). The WT and isolate M exhibited identical numbers of
215 plaques, suggesting this isolate does not exhibit equivalent resistance in plaque-based assays
216 to that seen in liquid culture experiments. However, the plaques of ICP1, ICP2, or ICP3 that
217 formed on isolate M were significantly cloudier than the WT strain, suggesting this isolate has
218 partial resistance to phage infection in these conditions (Fig. 5A). Despite no prior exposure to
219 ICP1 and ICP2, these ICP3 resistant isolates were able to survive predation indicating all three
220 phage require the O1 antigen for infection.
221
222 **A**

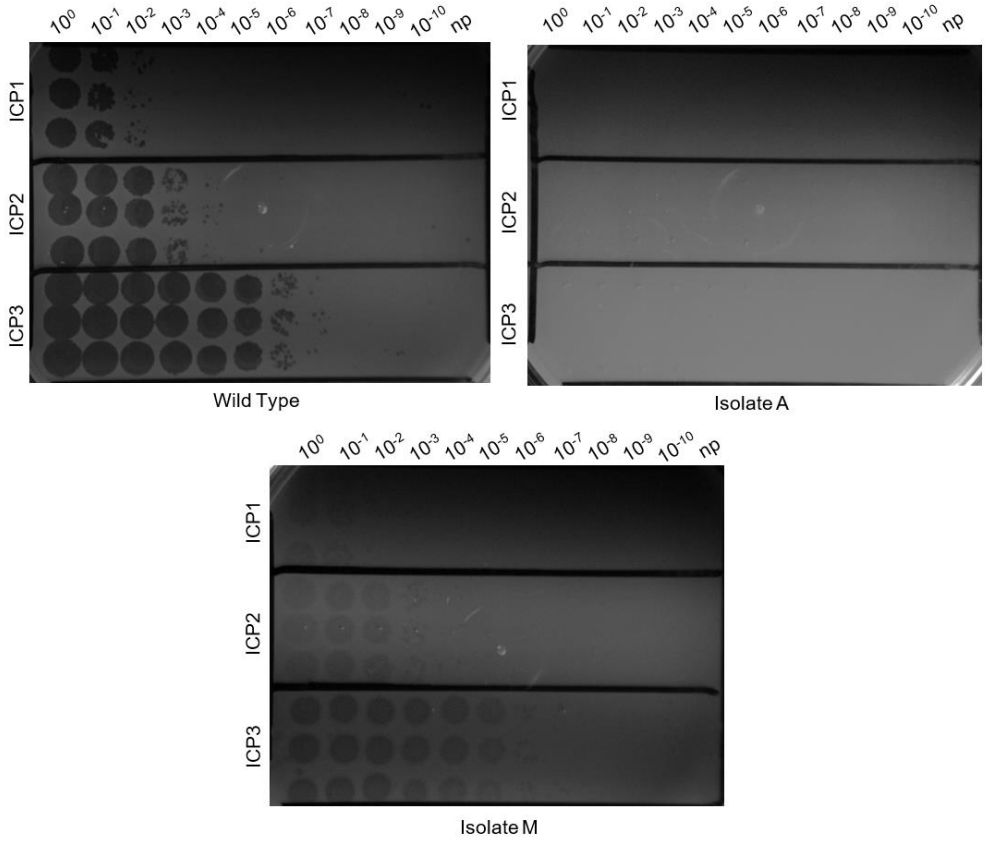

223

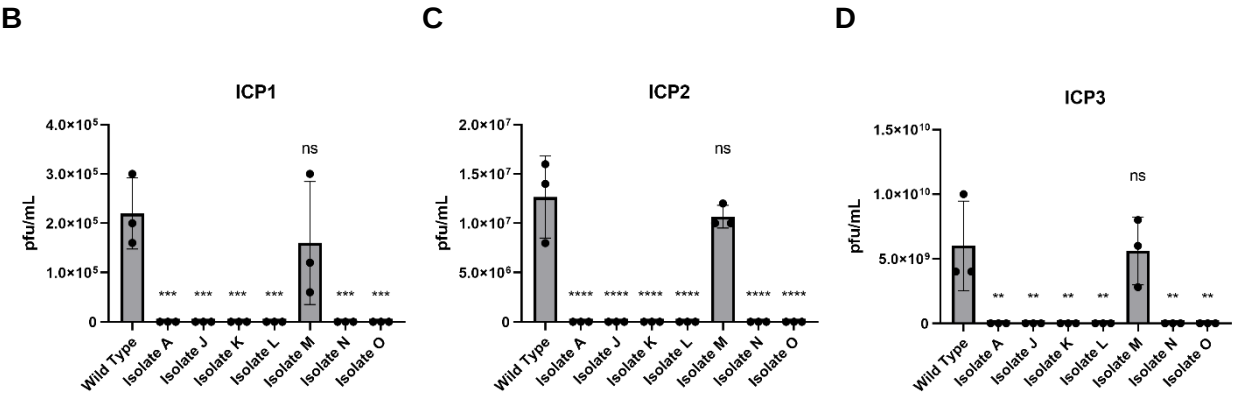

Figure 5: Efficiency of plaquing assay showing six isolates are pan-resistant to the three ICP phages.

Seven isolates that were resistant to ICP3 in liquid culture were challenged with the three ICP phages on solid media. (A) A WT host is shown as a control on the top left. Isolate A, a representative recovery isolate, is shown on the top right. Isolate M is shown on the bottom depicting similar plaquing to WT but with a hazier phenotype. Dilutions used are shown across the top. np = no phage. (B-D) All three replicates are shown as dots and the bar indicates the mean. Error bars represent the standard deviation. One-Way ANOVA was performed with Dunnett's post-hoc test between each isolate and the naive host. Statistical significance is noted as follows: (ns) not significant, (*)$p < 0.05$, (**)$p < 0.01$, (***)$p < 0.001$, and (****)$p < 0.0001$.

Restoration of O1 antigen biosynthesis restores phage susceptibility

To ensure that phage resistance was due to the sequenced mutations, two representative isolates, A and J, were chosen and complemented by constructing inducible plasmids encoding *manB* and *wbeU*, respectively (Table I). Liquid infection assays compared the complemented strains and a deficient strain containing an empty vector. ICP1, ICP2, or ICP3 phage were added at time 0 with a MOI of 1.0 (Fig. 6). In each case, the resistant isolates containing the complemented plasmid exhibited significant phage killing after 1 hr whereas the corresponding empty vector control strains were unimpacted by phage addition. In each experiment, there was

also a significant growth defect prior to phage infection for isolate J (*wbeU,* +G) with the empty vector compared to the complemented strains while isolate A (*manB,* Δ11) with the empty vector exhibited decreased growth compared to the complemented strain in 1 of the 3 experiments (p = 0.0585) (Fig. 6). This result suggests that not only do these mutations confer resistance to ICP phage infection, they also negatively impact growth of *V. cholerae* in the conditions examined here.

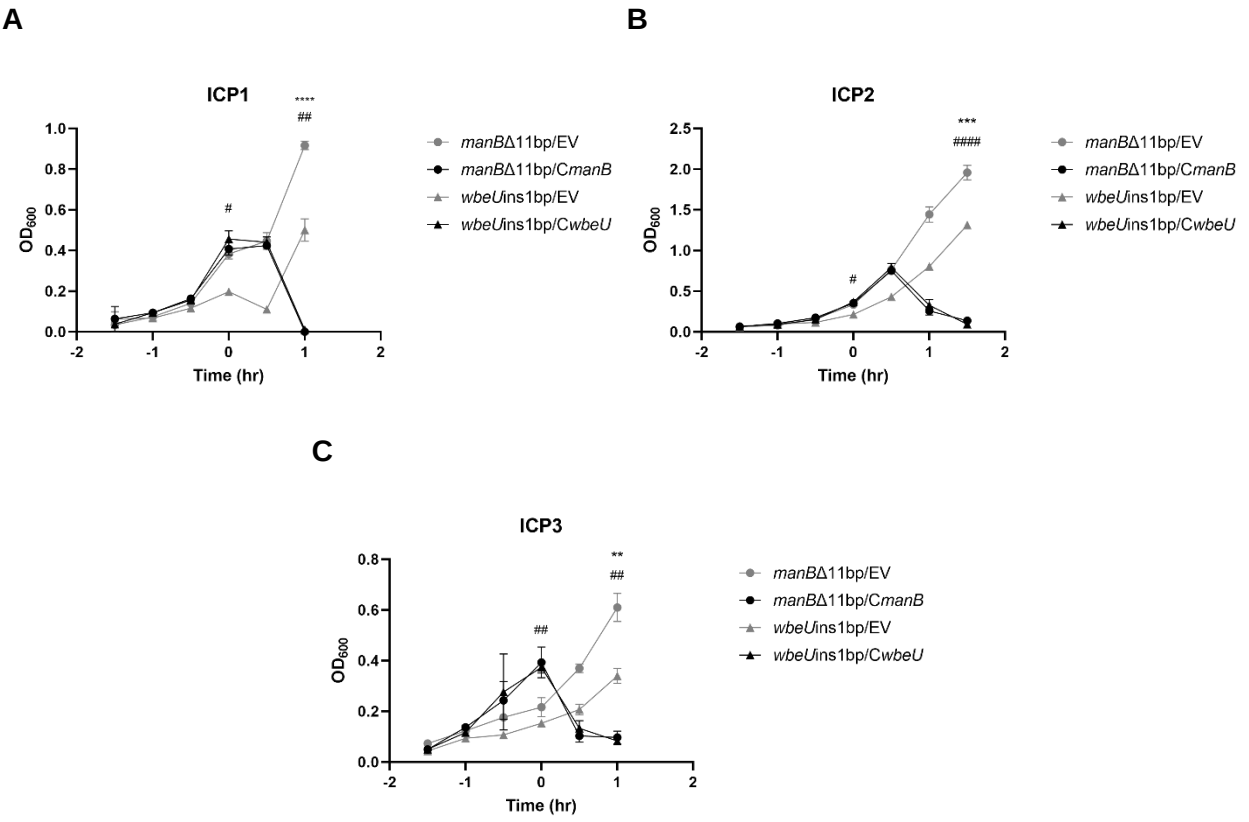

Figure 6: Complementation of mutated genes restores susceptibility phenotype. Strains with inducible plasmids containing the *manB* gene (C*manB*), the *wbeU* gene (C*wbeU*), or the empty vector (EV) control were challenged with ICP1 (A), ICP2 (B), and ICP3 (C) at 0 hours. Results are shown as the mean of three replicates with error bars as the standard deviation. Two-Way Repeated Measures ANOVA was performed with Tukey's post-hoc multiple comparisons tests between each strain. Significance is only shown at 0 hr and the final time

point. Statistical significance is noted as follows: asterisks (*) indicate significance between *manB*Δ11bp/EV and *manB*/C*manB*, pound signs (#) indicate significance between *wbeU*ins1bp/EV and *wbeU*ins1/C*wbeU*. Levels of significance are denoted by: (ns) not significant, (*)$p < 0.05$, (**)$p < 0.01$, (***)$p < 0.001$, and (****)$p < 0.0001$.

The ICP resistant mutants exhibit variable sensitivity to polymyxin B

In Gram-negative bacteria, the O antigen provides an outermost protective layer to various stresses and antimicrobials (18). Previous O1 biosynthesis mutants that were resistant to ICP1 infection exhibited increased sensitivity to the antimicrobial polymyxin B (14). We therefore performed a minimum inhibitory concentration assay to test if the seven O1 antigen ICP resistant mutants were likewise sensitive to polymyxin B (Fig. 7, Table 2). Indeed, all seven mutants exhibited increased sensitivity to polymyxin B relative to the WT strain, but only isolates K and O were significantly different from the WT strain (Table 2). Isolate M, which was less resistant to ICP infections in EOP assays, was the most like the WT strain with complete resistance to polymyxin B at 8 µg/mL whereas isolates K and O remained completely sensitive at this concentration. These results provide further evidence that these mutations disrupt O1 antigen biosynthesis although to varying degrees depending on the specific mutation.

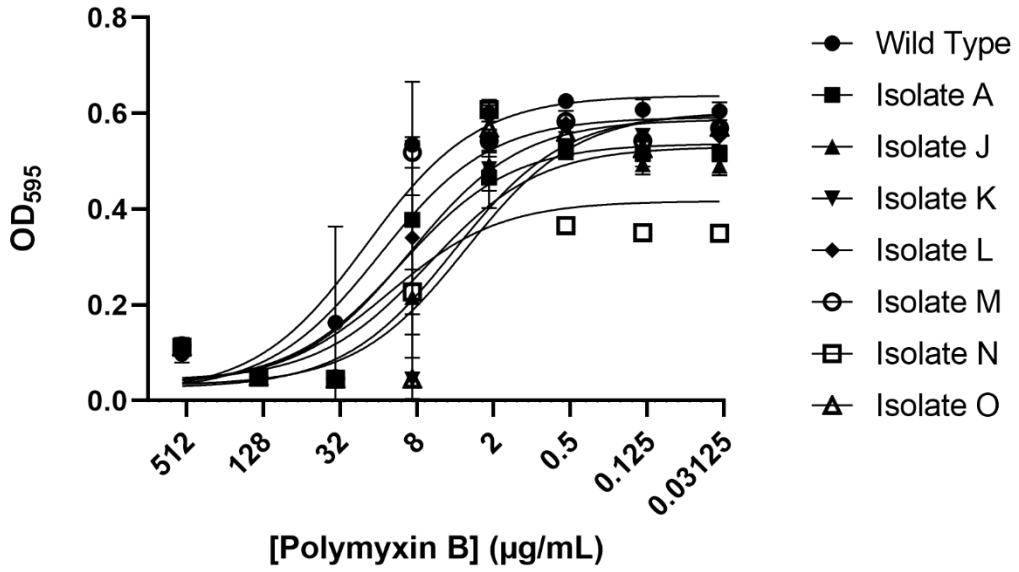

Figure 7: Mutant susceptibility to the antibiotic polymyxin B.

Lines of best fit were calculated using non-linear regression models to determine IC_{50}. Each condition includes three biological replicates, and error bars depict the standard deviation.

Table 2: Half-Maximal Inhibitory Concentrations of Phage Resistant Mutants to Polymyxin B

Isolate	IC_{50} (95% Confidence Interval) (µg/mL)
WT	19.7 (10.8 – 35.8)
A	10.6 (4.18 – 25.8)
J	6.42 (3.07 – 13.4)
K	3.26 (1.82 – 5.78)
L	8.95 (4.65 – 17.0)
M	15.5 (8.41 – 28.3)
N	13.1 (4.81 – 39.0)
O	4.08 (2.08 – 7.96)

Discussion

Our finding that *V. cholerae* cultures rebound after ICP3 infection through enrichment of escape mutants is consistent with the results of previous studies (3, 16, 26). Interestingly, all of these resistant mutants had defects in genes coding for enzymes that synthesize the O1 antigen. A putative pathway for the biosynthesis of the O1 antigen has been proposed by Stroeher *et al*, 1995 (27) with modifications by Chatterjee & Chaudhuri, 2004 (25) and Seed *et al*, 2012 (14). Three of our mutant strains in Table 1 had alterations to genes encoding perosamine synthesis enzymes. These include a frameshift deletion in the phosphomannomutase *manB* (Isolate A), a missense mutation in the GDP-mannose dehydratase *gmd* (Isolate M), and a frameshift deletion in the mannose-1 phosphate guanylyltransferase *manC* (Isolate N) (Table 1). Mutations that alter the function of these proteins prevent synthesis of the perosamine monomer in O1 antigen from being produced. *manB* mutations have been linked with *V. cholerae* ICP1 resistance, but not with resistance to ICP2 or ICP3 (26). Likewise, two mutations, one in-frame deletion (Isolate K) and one frameshift deletion (Isolate L), in the *wbeN* acyl-CoA reductase gene conferred pan-resistance to ICP phages (Table 1). The final isolates had a mutation in *wbeU* that is associated with LPS biosynthesis and *wbeM*, whose function in O1 antigen biosynthesis is unclear.

Given that the receptor for ICP1 has been previously identified as the O antigen, it is not surprising to see resistance among the isolates generated in this study. However, the requirement of the O1 antigen for infection by ICP2 has not been reported. OmpU was previously identified as a receptor for ICP2 (16), and it was recently determined that the ICP2 tail protein Gp23 interacts with OmpU (28, Fig. 8). OmpU was identified as the receptor of ICP2 from clinical stool samples by analyzing *V. cholerae* resistant to ICP2. These resistant mutants had mutations in *ompU* or *toxR,* a transcriptional activator of *ompU* (16). We speculate that mutations in the O1 antigen biosynthesis genes were not isolated in this study due to the significant *in vivo* cost for *V. cholerae* associated with the loss of O1 (14). Having multiple

receptors is not uncommon for phages, sometimes requiring both to be present for adsorption into the cell. This is exhibited by the *E. coli* phage K20 which utilizes LPS in addition to OmpF for infection perpetuation (29).

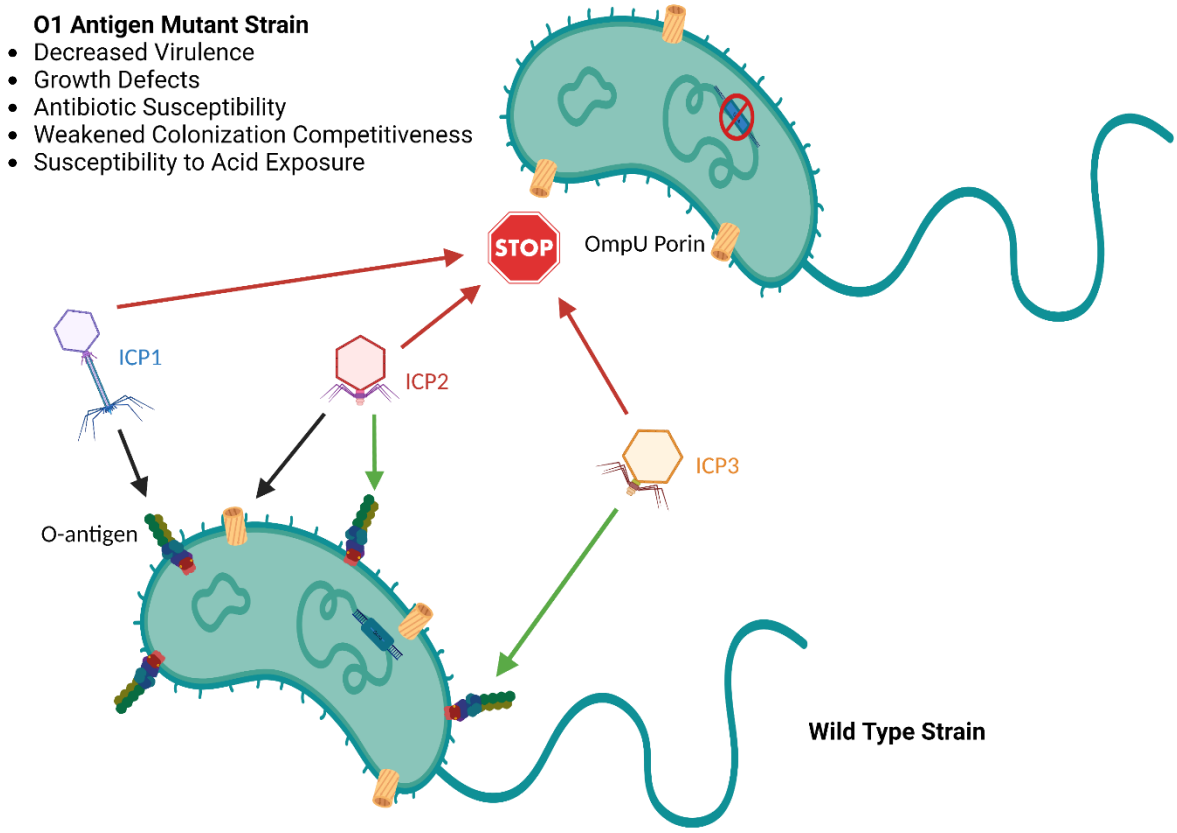

Figure 8: Model showing the known receptors of ICP phage.

This model shows a WT strain of *V. cholerae* on the bottom and a strain with a mutation in the O1 antigen biosynthesis pathway on top. The WT strain is able to produce both the O1 antigen and the Outer Membrane Porin U (OmpU) while the mutant can only produce the later. ICP1 is depicted as larger and a member of the *Myoviridae* family. ICP2 and ICP3 are depicted as smaller and members of the *Podoviridae* family. The three ICP phages and their previously known targets are shown as dark green arrows. The new targets identified by this study are shown by light green arrows.

This study is the first to report the O1 antigen is a receptor for ICP3 (Fig. 8). A study exploring VP4 phage which is genetically similar to ICP3 described its receptor in this same locus (13, 15). This study found mutations in *manB*, *manC*, *wbeU*, *wbeN*, and *wbeG*, which reinforce our findings here. Our isolation of seven independent mutations in O1 antigen biosynthesis and no other putative receptors may suggest that the O1 antigen is the sole receptor for ICP3. However, given that the target region for disruption of O1 antigen biosynthesis is large (Fig. 3), further studies with more saturating mutagenesis are required to conclusively test this hypothesis.

The results here raise an important question as to why these O1 antigen deficient *V. cholerae* lineages have not dominated environmentally since they provide pan-resistant to ICP1, ICP2, and ICP3 infection. Since LPS operates as a virulence factor within the human host, it is important for survival and replication in that niche (12). LPS mutants exhibit decreased competitiveness and ability to colonize the human gut compared to their wild type counterparts (30). There is additional evidence that the LPS protects against acid exposure which may be typical during human colonization (30). Furthermore, in our own studies, we observed decreased growth in O1 antigen biosynthesis mutants compared to their complemented counterparts in laboratory growth conditions and increased sensitivity to polymyxin B although it was only statistically significant in two mutants (Figs. 6 and 7). These collective results suggest that emergence of O1 antigen null mutants is not evolutionary favored due to the significant fitness cost of such mutations. This finding is consistent with previous studies that have similarly concluded that although isolation of phage receptor mutants is common during selection for phage resistance in laboratory conditions, such mutants are rarely seen in natural populations (31).

The E7946 El Tor strain encodes homopolymer nucleotide tracts in the genes *wbeL* and *manA,* which are required for O1 antigen biosynthesis, that mediate phase variable expression

of the O1 antigen leading to ICP1 phage resistance (14). It was postulated that such a system could lead to a strategy in which a segment of the population evolves resistance to ICP1 phage infection while maintaining the genetic potential to restore O1 for infection of the host. We did not isolate any mutations in *manA* or *wbeL*, and an analysis of the sequence of genes in the El Tor strain used here, C6706, showed that the polyA(A_9) tracts were conserved in *manA* but not in *wbeL.* This suggests that the loss of *manA* is not favored upon ICP3 selection.

As phages use cell surface proteins and molecules as receptors, an emerging concept is that resistance to phage infection may have the evolutionary tradeoff of antibiotic sensitivity. Such a tradeoff has been demonstrated in the *E. coli* phage U136B which uses the antibiotic efflux protein TolC as a receptor, as mutations that confer resistant to phage infection lead to increased antibiotic sensitivity (32). Evolving to recognize the O1 antigen as a receptor by all three ICP phage is a natural example of such a concept as any *V. cholerae* that gain resistance through loss of O1 have the tradeoff of loss of virulence and more sensitivity to host antimicrobials like polymyxin B. Therefore, evolution to use the O1 antigen as a receptor by ICP1, ICP2, and ICP3 has contributed to the evolutionary success of these lytic phage.

ACKNOWLEDGEMENTS

This research was supported and funded by NIH grants GM139537 and AI158433 to C.M.W. D.A.B. was supported by a Professorial Assistant fellowship from Michigan State University and the Norman E. & Hanna C. Kelker Research Scholarship and the Dietrich C. Bauer Scholarship from the Department of Microbiology and Molecular Genetics. We thank Andrew Camilli and Wai-Leung Ng at Tufts University for providing the ICP phage.

MATERIALS AND METHODS

Bacterial culturing and molecular biology

The WT culture is El Tor *V. cholerae* C6706:str2 (33). All cultures were grown in glass test tubes

(18 x 150 mm, Kimax) containing Luria-Bertani broth at 35°C with shaking, unless otherwise stated. Selection of plasmids utilized kanamycin at 100 µg/mL. The *manB* (pDAB1) and *wbeU* (pDAB2) complementation plasmids were generated using Gibson cloning. The gene inserts were generated from C6706:str2 with GoTaq 2x MasterMix using the primers (overhang, RBS, INSERT): 5'-acagcctcgacaggcctaggaggagctaaggaagctaaaGTGAAAGAGTTAACTTGTTTT-3' and 5'-gcttgctcaatcaatcaccgTTAAATATCCAATTTCTTAATTAATTTAGTAAG-3' (*manB*) 5'-acagcctcgacaggcctaggaggagctaaggaagctaaaATGCCATGGAAGACCTAC-3' and 5'-gcttgctcaatcaatcaccgTCAACAGACATTTCCGAAG3' (*wbeU*). These inserts were Gibson (New England Biolabs) cloned into an EcoRI/BamHI digested pEVS143 plasmid (34) using standard methodologies followed by Sanger sequencing to confirm the proper clone was generated. The empty vector and plasmids were conjugated from the *Escherichia coli* diaminopimelic acid auxotrophic strain BW29427 (K. Datsenko and B.L. Wanner, unpublished) into *V. cholerae* strains by mixing 25 µL of each culture overnight on an agar plate followed by selection on LB plates with kanamycin.

Liquid Infection Assays

30 µL of overnight cultures were back diluted into 3 mL of LB and allowed to grow until OD_{600} (0.20-0.50). Each culture was then infected with ICP1, ICP2, ICP3, or SM buffer (50 mM Tris-Cl + 100 mM NaCl + 8 mM $MgSO_4$). Phage stocks were maintained in filtered LB medium with trace chloroform and the pfu/mL of each phage was: ICP1 $9.2x10^5$ pfu/mL, ICP2 $1.3x10^8$ pfu/mL, and ICP3 $1.8x10^9$ pfu/mL. The amount of phage to add was determined by converting the optical density (OD) of the culture into an estimated viable cell count in *cfu/mL* using a quadratic regression equation generated from a previous growth curve: $cfu/mL = [1.4226 \times 10^9 \times (OD)^2] + [4.2981 \times 10^8 \times OD] - 2.2521 \times 10^6$. Following infection, the OD_{600} of cultures was remeasured every 0.25 hr. For the recovery experiments, cultures were allowed to recover for 24 hours. The recovery pools were collected and frozen in 20% glycerol at -80°C. The recovery

pools were then struck onto LB agar plates and individual isolates were used for reinfection. The same infection procedure was followed for the reinfection assays. For the liquid phage infection assays in Fig. 4, three independent overnight cultures of the WT or seven phage resistant isolates grown in 2 mL of LB were back diluted 1/100 in fresh LB and 100 µL was added to four wells into a clear 96-well plate (Costar). The plate was incubated at 35°C for 1.5 hours and to one well 1 µL of the ICP1, ICP2, or ICP3 phage stock was added. The OD_{595} was monitored every 0.25 hours in an Envision plate reader.

Efficiency of Plaquing Assays

Cultures of WT and resistant strains were grown overnight in LB and 250 µL was inoculated into 18 mL warm MMB (LB + 0.5% agar + 5 mM $MgCl_2$ + 5 mM $CaCl_2$ + 0.1 mM $MnCl_2$) at 55°C. The mixture was poured onto an empty plate (150 x 15 mm, Fisher Scientific) and allowed to solidify. Ten-fold serial dilutions of phage made in SM buffer were then spotted 5 µL in succession onto each strain along with one SM buffer spot as a negative control. This was performed in triplicate for each strain. Once plates were dried, they were allowed to incubate at 35°C overnight. Plaques were counted the next day to determine the efficiency of plaquing on each strain for each phage (ICP1, ICP2, and ICP3).

Whole Genome Sequencing and Analysis

Genomic extraction for the WT C6706:str2 strain and each of the resistant mutants was performed using Wizard Genomic DNA Purification Kit (Promega). The concentration of DNA was quantified using Nanodrop spectrophotometer (ND-1000). Samples were then sequenced at SeqCenter (Pittsburgh, PA). Results were processed by aligning each sample to the reference chromosomes of *V. cholerae* (NZ_CP046844 and NZ_CP046845) using *breseq* (35). Any mutations found in the WT strain as well as our resistant mutants were removed from consideration.

433

434 **Polymyxin B minimum inhibitory concentration**

435 Three independent overnight cultures of the WT and all seven resistant mutants were prepared
436 in 2 mL LB and diluted 1/100 in fresh media. A final volume of 150 µL of the diluted culture was
437 added to the well of a clear 96-well plate (Costar) and grown overnight at 35°C without shaking
438 in a humidity chamber with decreasing concentrations of polymyxin B starting at 555 mg/mL
439 followed by seven four-fold dilutions. The OD_{595} was measured using an Envision plate reader.

440

441 **REFERENCES**

442 1. Dalusi L, Lyimo TJ, Lugomela C, Hosea KMM, Sjöling S. 2015. Toxigenic *Vibrio cholerae*
443 identified in estuaries of Tanzania using PCR techniques. *FEMS Microbiol Lett* 362:fnv009.
444 2. Ali M, Nelson AR, Lopez AL, Sack DA. 2015. Updated Global Burden of Cholera in Endemic
445 Countries. *PLoS Negl Trop Dis* 9:e0003832.
446 3. Yen M, Cairns LS, Camilli A. 2017. A cocktail of three virulent bacteriophages prevents
447 *Vibrio cholerae* infection in animal models. *Nat Commun* 8:14187.
448 4. Kanungo S, Azman AS, Ramamurthy T, Deen J, Dutta S. 2022. Cholera. *The Lancet*
449 399:1429–1440.
450 5. Ganesan D, Gupta SS, Legros D. 2020. Cholera surveillance and estimation of burden of
451 cholera. *Vaccine* 38:A13–A17.
452 6. Yen M, Camilli A. 2017. Mechanisms of the evolutionary arms race between *Vibrio cholerae*
453 and Vibriophage clinical isolates. *Int Microbiol* 20:116–120.
454 7. Severin GB, Ramliden MS, Hawver LA, Wang K, Pell ME, Kieninger A-K, Khataokar A,
455 O'Hara BJ, Behrmann LV, Neiditch MB, Benning C, Waters CM, Ng W-L. 2018. Direct
456 activation of a phospholipase by cyclic GMP-AMP in El Tor *Vibrio cholerae*. *Proc Natl Acad*
457 *Sci USA* 115:E6048-E6055.

8. O'Hara BJ, Barth ZK, McKitterick AC, Seed KD. 2017. A highly specific phage defense system is a conserved feature of the *Vibrio cholerae* mobilome. *PLoS Genet* 13:e1006838.
9. Hsueh BY, Severin GB, Elg CA, Waldron EJ, Kant A, Wessel AJ, Dover JA, Rhoades CR, Ridenhour BJ, Parent KN, Neiditch MB, Ravi J, Top EM, Waters CM. 2022. Phage defence by deaminase-mediated depletion of deoxynucleotides in bacteria. *Nat Microbiol* 7:1210–1220.
10. Seed KD, Lazinski DW, Calderwood SB, Camilli A. 2013. A bacteriophage encodes its own CRISPR/Cas adaptive response to evade host innate immunity. *Nature* 494:489–491.
11. Boyd CM, Angermeyer A, Hays SG, Barth ZK, Patel KM, Seed KD. 2021. Bacteriophage ICP1: A Persistent Predator of *Vibrio cholerae*. *Annu Rev Virol* 8:285–304.
12. Seed KD, Bodi KL, Kropinski AM, Ackermann H-W, Calderwood SB, Qadri F, Camilli A. 2011. Evidence of a Dominant Lineage of *Vibrio cholerae*-Specific Lytic Bacteriophages Shed by Cholera Patients over a 10-Year Period in Dhaka, Bangladesh. *mBio* 2:e00334-10.
13. Barman RK, Chakrabarti AK, Dutta S. 2022. Screening of Potential *Vibrio cholerae* Bacteriophages for Cholera Therapy: A Comparative Genomic Approach. *Front Microbiol* 13:803933.
14. Seed KD, Faruque SM, Mekalanos JJ, Calderwood SB, Qadri F, Camilli A. 2012. Phase Variable O Antigen Biosynthetic Genes Control Expression of the Major Protective Antigen and Bacteriophage Receptor in *Vibrio cholerae* O1. *PLoS Pathog* 8:e1002917.
15. Xu J, Zhang J, Lu X, Liang W, Zhang L, Kan B. 2013. O Antigen Is the Receptor of *Vibrio cholerae* Serogroup O1 El Tor Typing Phage VP4. *J Bacteriol* 195:798–806.
16. Seed KD, Yen M, Shapiro BJ, Hilaire IJ, Charles RC, Teng JE, Ivers LC, Boncy J, Harris JB, Camilli A. 2014. Evolutionary consequences of intra-patient phage predation on microbial populations. *eLife* 3:e03497.

17. Reyes-Robles T, Dillard RS, Cairns LS, Silva-Valenzuela CA, Housman M, Ali A, Wright ER, Camilli A. 2018. *Vibrio cholerae* Outer Membrane Vesicles Inhibit Bacteriophage Infection. *J Bacteriol* 200:e00792-17.

18. Chatterjee SN, Chaudhuri K. 2006. Lipopolysaccharides of *Vibrio cholerae*: III. Biological functions. *Biochim Biophys Acta* 1762:1–16.

19. Mathur J, Waldor MK. 2004. The *Vibrio cholerae* ToxR-Regulated Porin OmpU Confers Resistance to Antimicrobial Peptides. *Infect Immun* 72:3577–3583.

20. Gupta P, Modgil V, Kant V, Kaur H, Narayan C, Mahindroo J, Verma R, Mohan B, Taneja N. 2022. Phenotypic and genotypic characterization of antimicrobial resistance in clinical isolates of *Vibrio cholerae* over a decade (2002-2016). *Indian J Med Microbiol* 40:24–29.

21. Miwanda B, Moore S, Muyembe J-J, Nguefack-Tsague G, Kabangwa IK, Ndjakani DY, Mutreja A, Thomson N, Thefenne H, Garnotel E, Tshapenda G, Kakongo DK, Kalambayi G, Piarroux R. 2015. Antimicrobial Drug Resistance of *Vibrio cholerae*, Democratic Republic of the Congo. *Emerg Infect Dis* 21:847–851.

22. Rodriguez-Gonzalez RA, Leung CY, Chan BK, Turner PE, Weitz JS. 2020. Quantitative Models of Phage-Antibiotic Combination Therapy. *mSystems* 5:e00756-19.

23. Hsueh BY, Waters CM. 2019. Combating Cholera. *F1000research* 8:589.

24. Bhandare S, Colom J, Baig A, Ritchie JM, Bukhari H, Shah MA, Sarkar BL, Su J, Wren B, Barrow P, Atterbury RJ. 2019. Reviving Phage Therapy for the Treatment of Cholera. The *J Infect Dis* 219:786–794.

25. Chatterjee SN, Chaudhuri K. 2004. Lipopolysaccharides of *Vibrio cholerae*. *Biochim Biophys Acta* 1690:93–109.

26. Silva-Valenzuela CA, Camilli A. 2019. Niche adaptation limits bacteriophage predation of *Vibrio cholerae* in a nutrient-poor aquatic environment. *Proc Natl Acad Sci USA* 116:1627–1632.

507 27. Stroeher UH, Karageorgos LE, Brown MH, Morona R, Manning PA. 1995. A putative
508 pathway for perosamine biosynthesis is the first function encoded within the *rfb* region of
509 *Vibrio cholerae* O1. *Gene* 166:33-42.
510 28. Lim ANW, Yen M, Seed KD, Lazinski DW, Camilli A. 2021. A Tail Fiber Protein and a
511 Receptor-Binding Protein Mediate ICP2 Bacteriophage Interactions with *Vibrio cholerae*
512 OmpU. *J Bacteriol* 203:e00141-21.
513 29. Silverman JA, Benson SA. 1987. Bacteriophage K20 requires both the OmpF porin and
514 lipopolysaccharide for receptor function. *J Bacteriol* 169:4830–4833.
515 30. Nesper J, Lauriano CM, Klose KE, Kapfhammer D, Kraiß A, Reidl J. 2001. Characterization
516 of *Vibrio cholerae* O1 El Tor *galU* and *galE* Mutants: Influence on Lipopolysaccharide
517 Structure, Colonization, and Biofilm Formation. *Infect Immun* 69:435–445.
518 31. Mutalik VK, Adler BA, Rishi HS, Piya D, Zhong C, Koskella B, Kutter EM, Calendar R,
519 Novichkov PS, Price MN, Deutschbauer AM, Arkin AP. 2020. High-throughput mapping of
520 the phage resistance landscape in *E. coli*. *PLoS Biol* 18:e3000877.
521 32. Burmeister AR, Fortier A, Roush C, Lessing AJ, Bender RG, Barahman R, Grant R, Chan
522 BK, Turner PE. 2020. Pleiotropy complicates a trade-off between phage resistance and
523 antibiotic resistance. *Proc Natl Acad Sci USA* 117:11207–11216.
524 33. Thelin KH, Taylor RK. 1996. Toxin-coregulated pilus, but not mannose-sensitive
525 hemagglutinin, is required for colonization by *Vibrio cholerae* O1 El Tor biotype and O139
526 strains. *Infect Immun* 64:2853–2856.
527 34. Dunn AK, Millikan DS, Adin DM, Bose JL, Stabb EV. 2006. New *rfp* - and pES213-Derived
528 Tools for Analyzing Symbiotic *Vibrio fischeri* Reveal Patterns of Infection and *lux* Expression
529 In Situ. *Appl Environ Microbiol* 72:802–810.
530 35. Deatherage DE, Barrick JE. 2014. Identification of Mutations in Laboratory-Evolved
531 Microbes from Next-Generation Sequencing Data Using *breseq*. *Methods Mol Biol*
532 1151:165-188.

533 36. Fallarino A, Mavrangelos C, Stroeher UH, Manning PA. 1997. Identification of additional
534 genes required for O-antigen biosynthesis in *Vibrio cholerae* O1. *J Bacteriol* 179:2147–
535 2153.
536 37. Pombo JP, Ebenberger SP, Müller AM, Wolinski H, Schild S. 2022. Impact of Gene
537 Repression on Biofilm Formation of *Vibrio cholerae*. *Front Microbiol* 13:912297.
538